

## Validation of the Global Relocatable Tide/Surge Model PCTides

PAMELA G. POSEY, RICHARD A. ALLARD, RUTH H. PRELLER, AND GRETCHEN M. DAWSON

*Naval Research Laboratory, Stennis Space Center, Mississippi*

(Manuscript received 5 October 2006, in final form 17 October 2007)

### ABSTRACT

The Naval Research Laboratory (NRL) has developed a global, relocatable, tide/surge forecast system called PCTides. This system was designed in response to a U.S. Navy requirement to rapidly produce tidal predictions anywhere in the world. The system is composed of a two-dimensional barotropic ocean model driven by tidal forcing only or in conjunction with surface wind and pressure forcing. PCTides is unique in its ability to forecast tidal parameters for a user-specified latitude/longitude domain easily and quickly, and is especially useful in areas where observations are nonexistent. PCTides provides short-term (daily to weekly) predictions of water-level elevation and depth-averaged ocean currents. The system has been tested in numerous regions and validated against observations collected in conjunction with several navy exercises.

### 1. Introduction

The ebb and flow of tidal waters are of importance for a wide range of military applications including mission planning, amphibious landings (e.g., the D-Day invasions at Normandy, France; and Inchon, South Korea), ship routing, navigation through harbors, bathymetry processing (i.e., the removal of tidal effects from sounding data), and the operation of unmanned underwater vehicles in shallow water. Tidal currents can affect the positioning and/or movement of subsurface mines and the performance of U.S. Navy sea, air, or land (SEAL) swimmers.

The U.S. Navy's globally relocatable tidal prediction model, PCTides, was developed to fill a void in the navy's global tide forecasting capability. Previously, tidal forecasts available to the navy were confined to coastal locations where water-level data were available. This restricted tidal forecasts to small areas between tidal stations. In addition, these forecasts did not include the effects of wind (surge), which can play a substantial role in water-level prediction.

PCTides was developed as a global tide-forecasting system that can be set up rapidly for any user-specified

location(s) to predict the water-level elevation and depth-averaged ocean currents. In addition, PCTides can assimilate the local meteorological effects of wind and surface pressure gradients, which typically play a role in water-level prediction. PCTides was specifically designed to produce daily to weekly forecasts of tidal conditions; however, longer predictions (e.g., months) can be made for military mission planning as well as for estimating optimal times for deployment of instrumentation, etc. The global, rapidly relocatable tide/surge forecast system is implemented on Windows operating systems (e.g., XP) running in a DOS mode as well as on UNIX and LINUX platforms.

Section 2 of this paper describes the PCTides system, and section 3 presents a discussion of validation tests performed at various worldwide locations. A summary and conclusions are presented in section 4.

### 2. The PCTides system

The PCTides system has a two-dimensional (2D) barotropic ocean model as its core component (Fig. 1). PCTides uses this barotropic ocean model to predict both depth-averaged currents and sea level heights on or near continental shelves (Preller et al. 2002). It contains a wetting and drying algorithm for the simulation of coastal flooding due to tides or storm surge. The model is driven by tidal forcing and, if desired, atmospheric surface wind and pressure.

---

*Corresponding author address:* Pamela G. Posey, Naval Research Laboratory, Code 7322, Building 1009, Room C132, Stennis Space Center, MS 39529.  
E-mail: posey@nrlssc.navy.mil

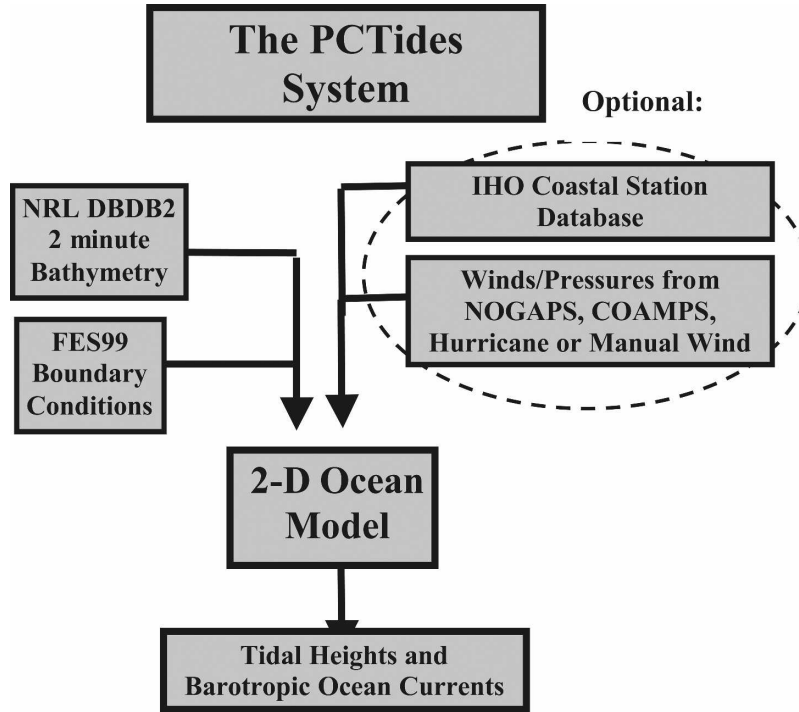


FIG. 1. The PCTides system components.

### a. The PCTides Ocean Model

PCTides uses the following shallow-water equations to define the depth-averaged current [Eqs. (1)–(2)] and the sea surface elevation [Eq. (3)]:

$$\begin{aligned} \frac{\partial U}{\partial t} = & fV - mg \frac{\partial \zeta}{\partial x} - \frac{m}{\rho_w} \frac{\partial P}{\partial x} - m \left( U \frac{\partial U}{\partial x} + V \frac{\partial U}{\partial y} \right) \\ & + \frac{1}{\rho_w H} \left( \tau_{sx} - \tau_{bx} - \frac{\partial S_{xx}}{\partial x} - \frac{\partial S_{xy}}{\partial y} \right) - \nu \nabla^2 U, \end{aligned} \quad (1)$$

$$\begin{aligned} \frac{\partial V}{\partial t} = & -fU - mg \frac{\partial \zeta}{\partial y} - \frac{m}{\rho_w} \frac{\partial P}{\partial y} - m \left( U \frac{\partial V}{\partial x} + V \frac{\partial V}{\partial y} \right) \\ & + \frac{1}{\rho_w H} \left( \tau_{sy} - \tau_{by} - \frac{\partial S_{yx}}{\partial x} - \frac{\partial S_{yy}}{\partial y} \right) - \nu \nabla^2 V, \end{aligned} \quad (2)$$

$$\frac{\partial \zeta}{\partial t} = -m^2 \left[ \frac{\partial}{\partial x} \left( \frac{UH}{m} \right) + \frac{\partial}{\partial y} \left( \frac{VH}{m} \right) \right], \quad (3)$$

where  $U$  and  $V$  are the depth-averaged currents in the  $x$  and  $y$  directions, respectively;  $H$  is the total depth;  $\zeta$  is the sea surface elevation;  $f$  is the Coriolis parameter;  $m$  is the map factor (a scaling factor dependent on the

chosen map projection of the model grid);  $g$  is the acceleration due to gravity;  $P$  is the atmospheric surface pressure;  $\rho_w$  is the water density;  $\nu$  is the coefficient of lateral eddy diffusion;  $\tau_{bx}$  and  $\tau_{by}$  are the bottom frictional stress;  $\tau_{sx}$  and  $\tau_{sy}$  are the surface wind stress in the  $x$  and  $y$  directions; and  $S_{xx}$ ,  $S_{yy}$ ,  $S_{xy}$ , and  $S_{yx}$  represent surface wave radiation stresses.

The surface wind stress components are computed using the quadratic relationship:

$$\tau_{sx} = C_D \rho_a |\mathbf{u}_a| u_a, \quad \tau_{sy} = C_D \rho_a |\mathbf{u}_a| v_a, \quad (4)$$

where  $|\mathbf{u}_a| = (u_a^2 + v_a^2)^{1/2}$ ,  $u_a$  and  $v_a$  are the horizontal components of wind velocity at anemometer height,  $\rho_a$  is the density of air, and  $C_D$  is the drag coefficient based on Smith and Banke (1975), which is expressed as follows:

$$\begin{aligned} C_D = & [0.63 + 0.066|\mathbf{u}_a|] \times 10^{-3} & |\mathbf{u}_a| < 25 \text{ m s}^{-1} \\ C_D = & [2.28 + 0.033(|\mathbf{u}_a| - 25)] \times 10^{-3} & |\mathbf{u}_a| \geq 25 \text{ m s}^{-1}. \end{aligned} \quad (5)$$

The bottom stress is represented by a Manning's  $n$  depth-dependent friction relation (Signell and Butman 1992):

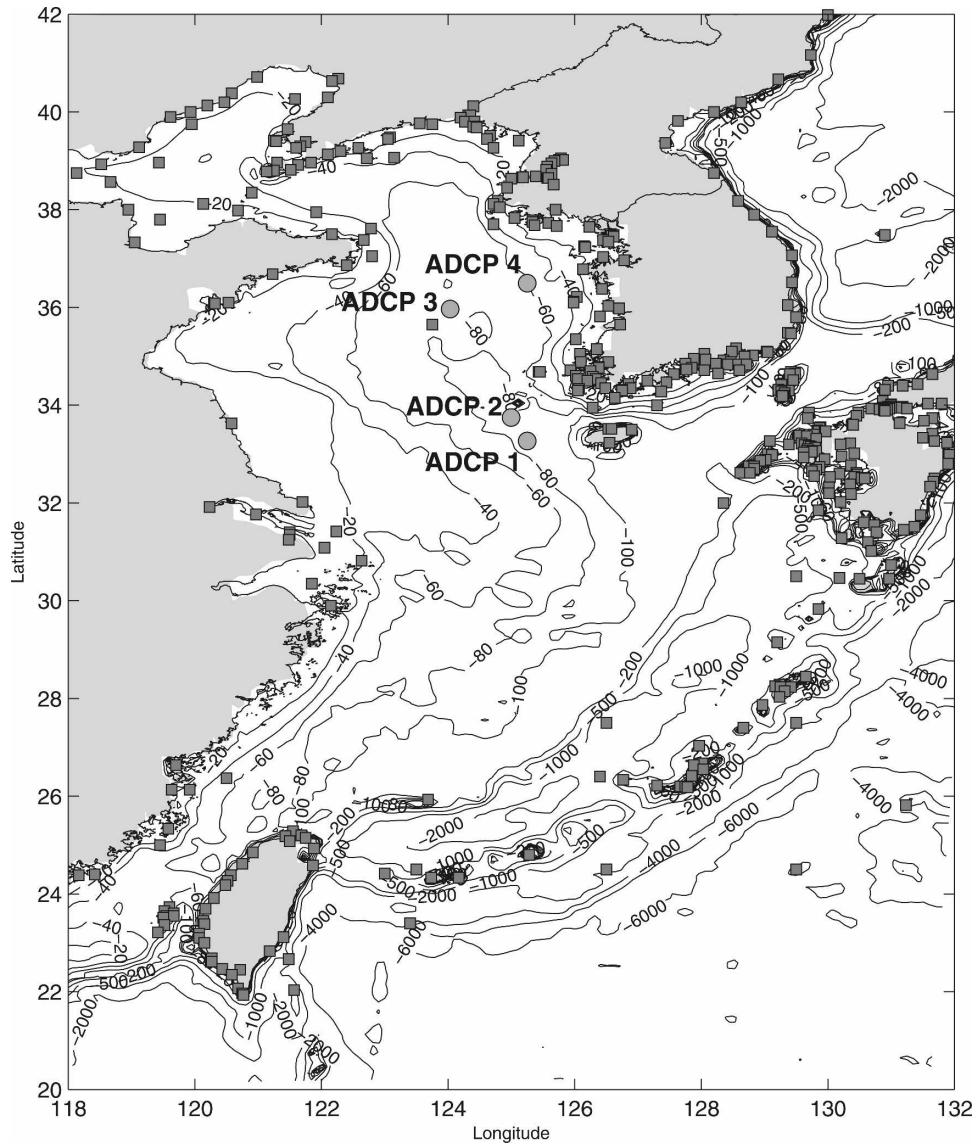


FIG. 2. Bathymetry (m) of the Yellow Sea. Squares indicate the IHO station locations and circles indicate the location of the ADCPs during September 1995.

$$\begin{aligned}\tau_{bx} &= \rho_w \frac{gn^2}{(H + \zeta)^{1/3}} (U^2 + V^2)^{1/2} U, \\ \tau_{by} &= \rho_w \frac{gn^2}{(H + \zeta)^{1/3}} (U^2 + V^2)^{1/2} V,\end{aligned}\quad (6)$$

where  $n$  has the value 0.03. This formulation ensures that the drag coefficient increases with decreasing water depth and is applied to water depths greater than 1 m. In extremely shallow water and over land points that become inundated, the bottom drag coefficients can be specified at each grid point according to the terrain type.

Equations (1)–(3) are solved on an Arakawa C grid (Messinger and Arakawa 1976) using a three-level, split-explicit finite-difference scheme as described in Hubbert et al. (1990). The continuity equation and the gravity wave and Coriolis terms in the momentum equations are solved with the shortest time step using the forward–backward method. The nonlinear advective terms are solved with an intermediate time step using the two-time-level method of Miller and Pearce (1974). The surface wind stress, bottom friction stress, and atmospheric pressure terms are solved with the longest time step using a backward-implicit method. This split-explicit approach is very efficient for oceano-

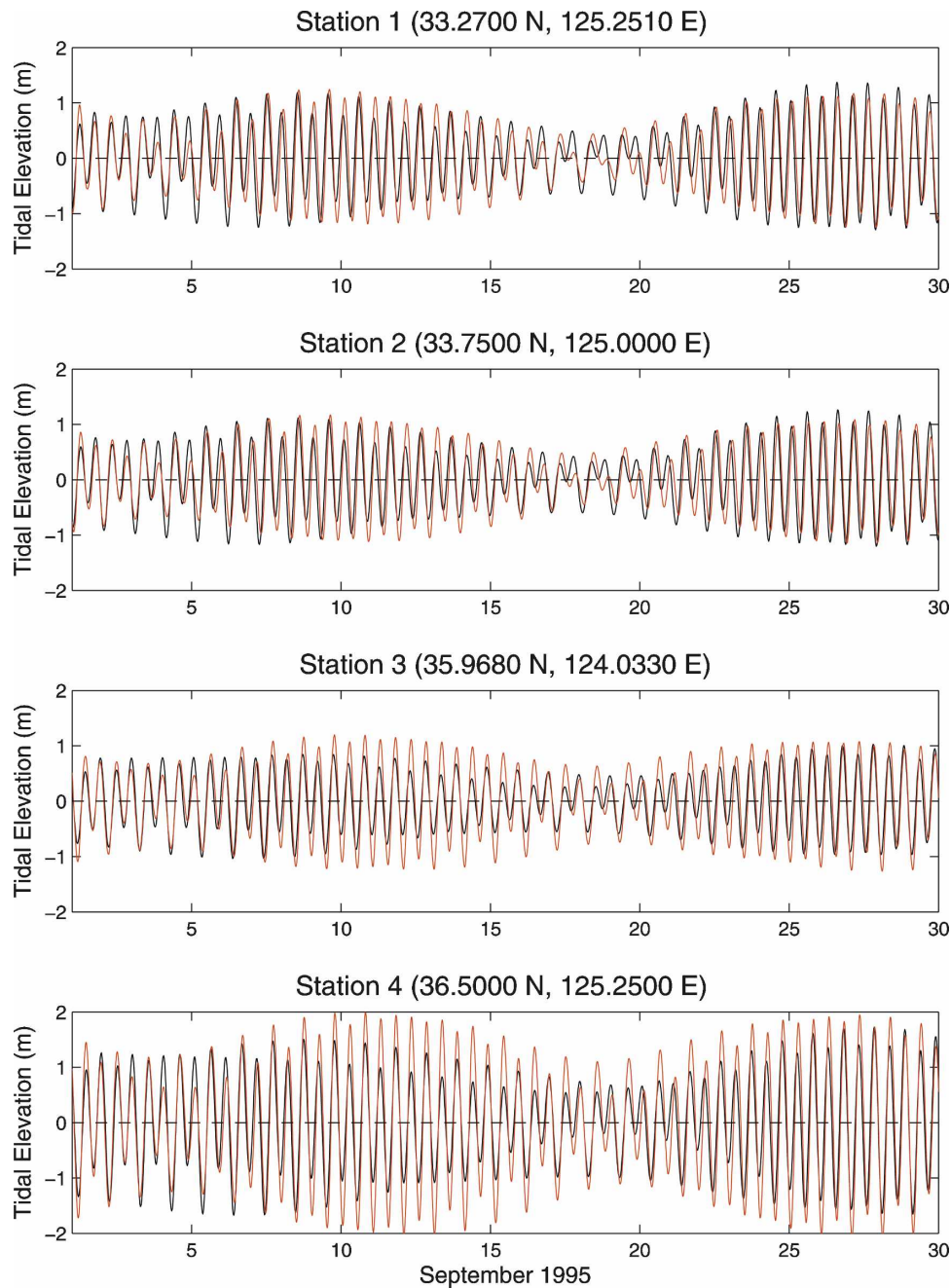


FIG. 3. Yellow Sea PCTides water-level elevation forecasts (red; m) with data assimilation vs the ADCP observations (black) at stations 1–4 for the period 1–30 Sep 1995.

graphic models with a free surface because of the large disparity between advective and gravity wave phase speeds in deep water.

Surface meteorological forcing is applied via the wind stress and surface pressure gradient terms in Eqs. (1)–(3) at all nonland model grid points in the computational domain. Tidal and meteorological forcing at the lateral boundaries is specified by the incremental

displacement of the water surface due to changes in tidal height and atmospheric barometric displacement. The lateral boundary conditions are applied using a one-way nesting technique. Tidal elevation boundary values are applied with decreasing intensity from the boundary to some specified number of model grid points ( $n_{\max} \sim 12$ ) into the domain according to the following equation:

$$\phi = (1 - \alpha)\phi_p + \alpha\phi_b, \quad (7)$$

where  $\phi_p$  is the model-predicted value,  $\phi_b$  is the prescribed boundary value, and  $\alpha$  is varied according to a cosine function such that

$$\alpha = 0.5[\cos\pi(1 - n/n_{\max}) + 1], n = 1, n_{\max}. \quad (8)$$

Under any prescribed boundary forcing, the model is initialized by setting velocities to zero and interpolating the global Finite Element Solutions version 99 (FES99) (Lefevre et al. 2002) elevation field to the model grid. A spinup period is used to allow the effects of the initial conditions and boundary forcing to propagate throughout the computational domain. Sensitivity studies have determined that the spinup time needed for PCTides using wind and tidal forcing is 24 h and is 12 h when wind forcing is not used.

#### b. PCTides configuration

PCTides was developed as a stand-alone, global, tidal prediction system and, as such, contains all of the necessary global databases. These databases include bathymetry, tidal boundary forcing data, and tidal station data. PCTides uses a 2-min global bathymetry database developed by Naval Research Laboratory (NRL) called NRL Digital Bathymetric database 2 min (DBDB2) (see [http://www7320.nrlssc.navy.mil/DBDB2\\_WWW/](http://www7320.nrlssc.navy.mil/DBDB2_WWW/)). This database is derived from a number of sources including the U.S. Naval Oceanographic Office (NAVOCEANO) global dataset (DBDBV, available online at [http://gcmd.nasa.gov/records/GCMD\\_DBDBV.html](http://gcmd.nasa.gov/records/GCMD_DBDBV.html)), the Smith and Sandwell global dataset, the Data Assimilation and Model Evaluation Experiments (DAMEE) North Atlantic data, the International Bathymetric Chart of the Arctic Ocean (IBCAO) data, the Australian Bathymetric and Topographic (ABTG) data, and regional datasets from the Gulf of Mexico and Yellow Sea. In addition, an appropriately formatted, user-supplied bathymetry can be blended with the default bathymetry to create bathymetry for highly resolved grids.

The FES99 global tidal database, which provides tidal data for the open boundaries of PCTides, contains tidal harmonics for nine constituents ( $M_2$ ,  $S_2$ ,  $N_2$ ,  $K_2$ ,  $K_1$ ,  $O_1$ ,  $P_1$ ,  $Q_1$ , and  $2N_2$ ). Although the total tide is defined by a much larger set of constituents, these nine provide a large percentage of the total tide. The FES99 database has  $0.25^\circ$  resolution and was derived by the assimilation of approximately 700 tide gauge and 687 Ocean Topography Experiment (TOPEX)/Poseidon altimetry measurements.

TABLE 1a. Statistics of water-level elevation (m) and phase (min) for PCTides Yellow Sea predictions compared to observations.

	With data assimilation						
	Water-level elevation					Phase	
	RMSE	$\sigma_{\text{Mod}}$	$\sigma_{\text{Obs}}$	$R$	SS	$R_p$	Lag
Location 1	0.44	0.52	0.63	0.72	0.51	0.95	-84
Location 2	0.43	0.55	0.58	0.72	0.47	0.95	-84
Location 3	0.30	0.60	0.50	0.87	0.65	0.94	-48
Location 4	0.49	1.06	0.84	0.89	0.66	0.94	-36
Average	0.42	0.68	0.64	0.80	0.57	0.95	63*
	Without data assimilation						
	RMSE	$\sigma_{\text{Mod}}$	$\sigma_{\text{Obs}}$	$R$	SS	$R_p$	Lag
	RMSE	$\sigma_{\text{Mod}}$	$\sigma_{\text{Obs}}$	$R$	SS	$R_p$	Lag
Location 1	0.46	0.63	0.63	0.73	0.46	0.95	-84
Location 2	0.43	0.63	0.58	0.75	0.46	0.95	-84
Location 3	0.30	0.50	0.50	0.82	0.64	0.94	-60
Location 4	0.51	0.87	0.84	0.82	0.62	0.94	-60
Average	0.43	0.66	0.64	0.78	0.55	0.95	72*

The asterisk (\*) denotes absolute mean.

PCTides utilizes tide station data from the International Hydrographic Office (IHO) database (IHO 1988) for model validation and/or data assimilation. The IHO database in PCTides includes tidal data for approximately 4500 tide stations.

PCTides was developed to generate daily to weekly forecasts of water-level elevations and tidally driven currents and may include wind-driven effects. When wind is not included, the forecasts may be for any future time—next week or next year. If wind is included, the forecast corresponds to the time period of wind forcing. For most navy applications, wind and surface pressure are obtained from the U.S. Navy's Operational Global Atmospheric Prediction System (NOGAPS) (Hogan and Rosmond 1991) or the Coupled Ocean Atmosphere Mesoscale Prediction System (COAMPS) (Hodur 1997), with grid resolutions of  $0.5^\circ$  and  $0.2^\circ$ , respectively. These real-time operational wind and surface fields are available via the navy's Metcast system (<http://www.metnet.navy.mil/Metcast>), which allows a user to request specific, real-time, atmospheric forecast products. A second source of wind in the PCTides system is provided by a hurricane model (Holland 1980), which produces time-varying hurricane wind fields based on a prescribed track, minimum surface pressure, and radius of maximum winds. PCTides test cases using these hurricane winds have been documented for Hurricane Isabel (Preller et al. 2005) and Hurricane Katrina (Blain et al. 2007). A third source of wind in PCTides is the manual input of a constant value for wind speed and direction over the entire domain, which can

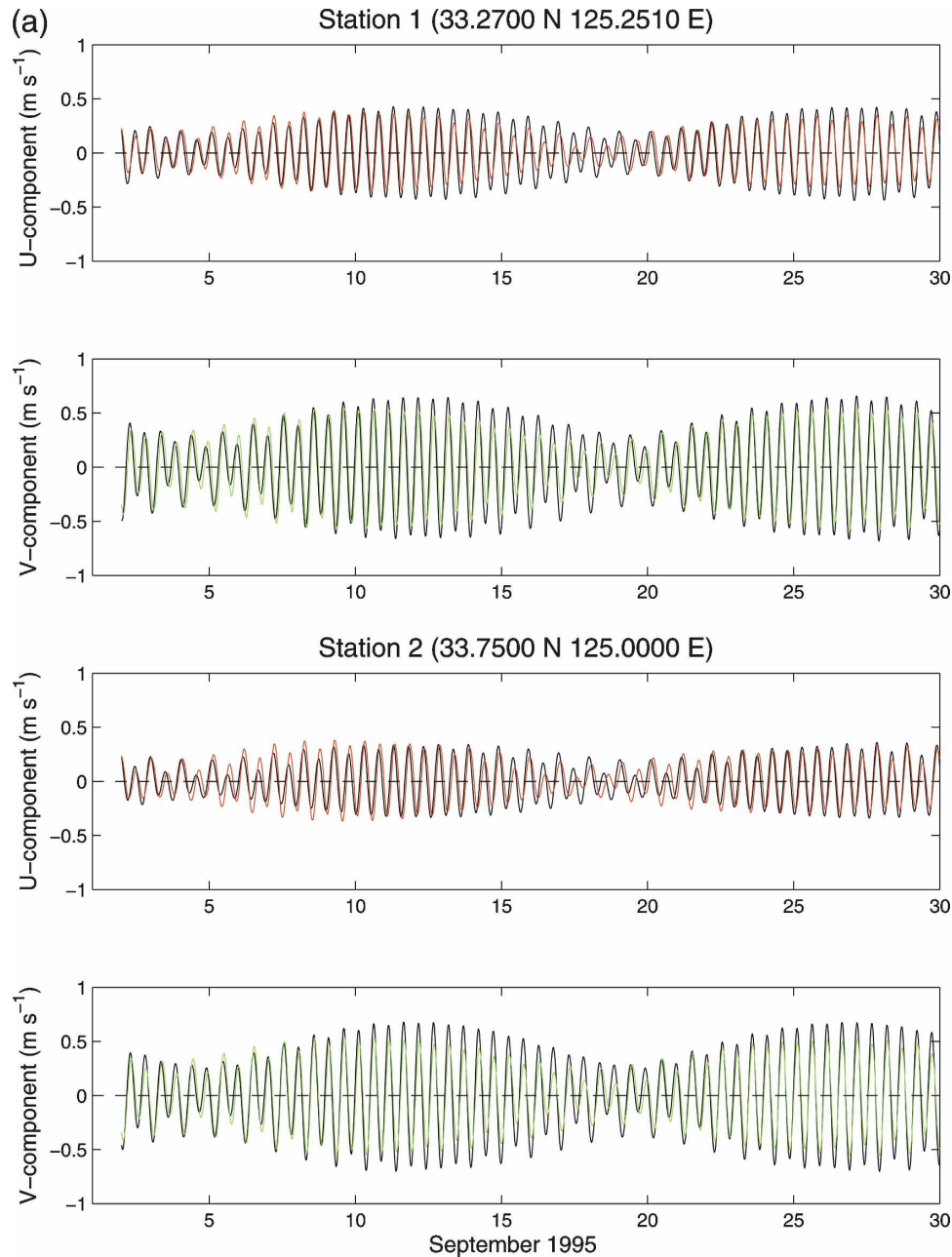


FIG. 4. (a) Yellow Sea PCTides depth-averaged tidal current forecasts ( $u$  and  $v$  components;  $\text{m s}^{-1}$ ) with data assimilation vs the depth-averaged ADCP observations (black) at stations 1 and 2 for the period 1–30 Sep 1995. (b) Yellow Sea PCTides depth-averaged tidal current forecasts ( $u$  and  $v$  components;  $\text{m s}^{-1}$ ) with data assimilation vs the depth-averaged ADCP observations (black) at stations 3 and 4 for the period 1–30 Sep 1995.

vary temporally but not spatially. This is useful in the case where a single, local wind record is available. It is also possible to run PCTides with atmospheric forcing from other meteorological models; however, existing software would have to be modified to process the new data type.

### c. PCTides data assimilation

To improve the simulation of tidally forced dynamics, software was built into PCTides to (optionally) nudge the model solution to tidal heights predicted using data from IHO tidal stations within the model do-

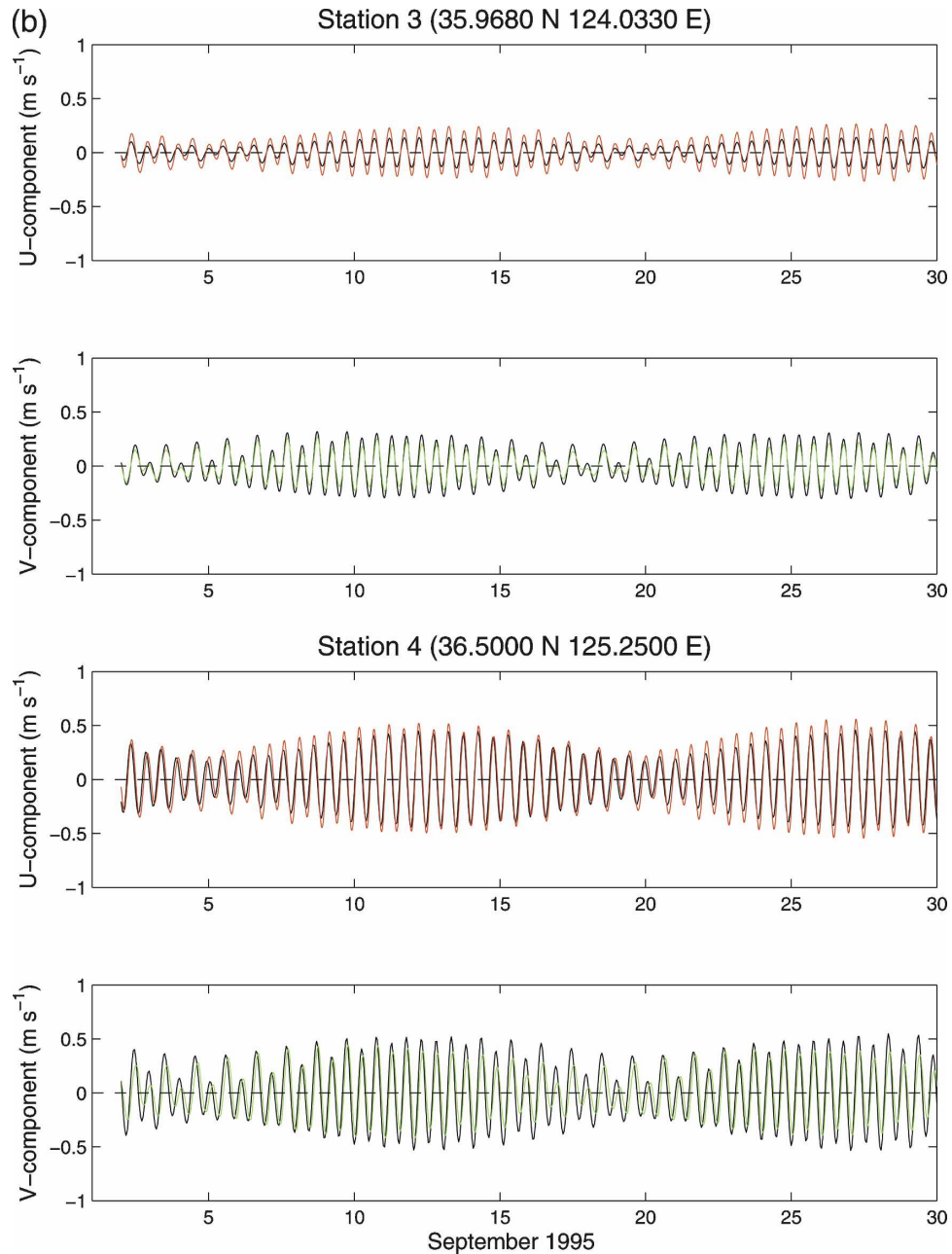


FIG. 4. (Continued)

main. The nudging method is based on deriving a new solution at grid points near each tidal station from a weighted combination of the model solution and the station observations. The weighting function is calculated from the product of a defined weighting constant and the following equation:

$$\beta = \cos(D\pi/d_{\max}) + 1, \quad (9)$$

where  $D$  is the distance from the grid point to the observation and  $d_{\max}$  is the radius of influence, which is

defined as 40 km. Figure 2 shows an example of IHO locations for the Yellow Sea region. Global IHO tidal constituent data are stored in ASCII format, and new datasets such as the TOPEX/Poseidon altimetry data, formatted appropriately, can easily be incorporated into the PCTides tidal dataset. PCTides has been tested with and without data assimilation. In some locations with open coastlines, the model performs well without data assimilation. However, in locations with more complex coastal geometry and bathymetry, data assi-

TABLE 1b. Statistics of tidal  $u$  and  $v$  components ( $\text{m s}^{-1}$ ) and phase (min) for PCTides Yellow Sea predictions compared to observations.

	With data assimilation													
	$U$ ( $\text{m s}^{-1}$ )					$U$ phase		$V$ ( $\text{m s}^{-1}$ )					$V$ phase	
	RMSE	$\sigma_{\text{Mod}}$	$\sigma_{\text{Obs}}$	$R$	SS	$R_p$	Lag (min)	RMSE	$\sigma_{\text{Mod}}$	$\sigma_{\text{Obs}}$	$R$	SS	$R_p$	Lag (min)
Location 1	0.10	0.19	0.23	0.90	0.81	0.97	-48	0.17	0.30	0.35	0.88	0.77	0.98	-60
Location 2	0.11	0.18	0.18	0.81	0.62	0.95	-72	0.13	0.29	0.37	0.95	0.87	0.98	-36
Location 3	0.06	0.13	0.07	0.99	0.44	0.99	-12	0.05	0.12	0.16	0.98	0.91	0.99	-12
Location 4	0.10	0.28	0.24	0.94	0.82	0.99	-36	0.16	0.22	0.28	0.81	0.66	0.98	-72
Average	0.09	0.20	0.18	0.91	0.67	0.98	42*	0.13	0.23	0.29	0.91	0.80	0.98	45*
	Without data assimilation													
	$U$ ( $\text{m s}^{-1}$ )					$U$ phase		$V$ ( $\text{m s}^{-1}$ )					$V$ phase	
	RMSE	$\sigma_{\text{Mod}}$	$\sigma_{\text{Obs}}$	$R$	SS	$R_p$	Lag (min)	RMSE	$\sigma_{\text{Mod}}$	$\sigma_{\text{Obs}}$	$R$	SS	$R_p$	Lag (min)
Location 1	0.16	0.18	0.23	0.69	0.46	0.96	-96	0.19	0.27	0.35	0.83	0.69	0.97	-60
Location 2	0.20	0.19	0.18	0.43	-0.02	0.96	-132	0.20	0.28	0.37	0.85	0.71	0.97	-60
Location 3	0.05	0.06	0.07	0.76	0.57	0.97	-84	0.06	0.17	0.16	0.95	0.88	0.98	-36
Location 4	0.18	0.18	0.24	0.66	0.43	0.96	-96	0.21	0.25	0.28	0.70	0.45	0.96	-96
Average	0.15	0.15	0.18	0.64	0.36	0.96	102*	0.17	0.24	0.29	0.83	0.66	0.97	63*

The asterisk (\*) denotes absolute mean.

lation often improves the solution. A previous study by Blain (1997) showed that the inclusion of coastal tide data can improve the accuracy of both coastal and deep-water tidal prediction.

#### d. PCTides execution and output

A typical 48-h forecast with a grid resolution of 5–10 km takes approximately 2–10 min to run using an Intel Core 2 CPU 6600 using 2.4 GHz with 3.00 GB of RAM. PCTides produces 2D output fields of water-level elevation and depth-averaged ocean currents at each model grid point. In addition, water-level elevation and current data can be saved at user-selected locations with a minimum output frequency of 10 min. The output can be viewed as an ASCII file or plotted as a time series.

### 3. PCTides validation

PCTides has been tested in over 15 regions around the globe (Posey et al. 2006). However, only a small subset of these comparisons is discussed here. Statistical evaluations were performed on the PCTides predictions by comparison with available data, including acoustic Doppler current profilers (ADCPs), bottom-mounted pressure sensors, and National Oceanic and Atmospheric Administration (NOAA) and IHO station data. The error statistics used include root-mean-square error (RMSE), standard deviation ( $\sigma$ ), correlation coefficient ( $R$ ), and skill score (SS) (Kara et al. 2003). The cross-correlation function ( $R_p$ ) (Jenkins and Watts 1969) was applied to the tidal phase for elevation

and velocity. The model's SS is computed from the following equation:

$$\text{SS} = R^2 - [R - (\sigma_y/\sigma_x)]^2 - [Y - X]/\sigma_x]^2, \quad (10)$$

where  $X$  is the mean of the data values;  $Y$  is the mean of the model values; and  $\sigma_x$  and  $\sigma_y$  are the standard deviation of the data and model values, respectively. An SS of 1.0 indicates a perfect PCTides prediction, and a negative SS indicates that PCTides may have normalized amplitudes larger than the correlation or large biases in the mean (Murphy and Epstein 1989).

To illustrate the accuracy of the system, the following section describes three major areas where PCTides have been validated as well as two additional cases of PCTides used with (Office of Naval Research) ONR- and (North Atlantic Treaty Organization) NATO-funded field experiments.

#### a. Yellow Sea region

Accurate prediction of water-level elevations and currents is a challenging task in the Yellow Sea because of complex bathymetry and coastal geometry. The sea is shallow with depths ranging from 90 m along the interior trough to  $\sim 20$  m within 50 km of the coast. Tidal amplitudes vary greatly in the Yellow Sea, with high ranges ( $\sim 9$  m) observed near Inchon. During the early 1990s, NAVOCEANO deployed four bottom-mounted ADCP moorings in the Yellow Sea (Fig. 2). A 30-day time series (1–30 September 1995) of velocity and pressure gauge data from the four stations was compared against two PCTides model forecasts without surface forcing. One of the forecasts assimilated IHO

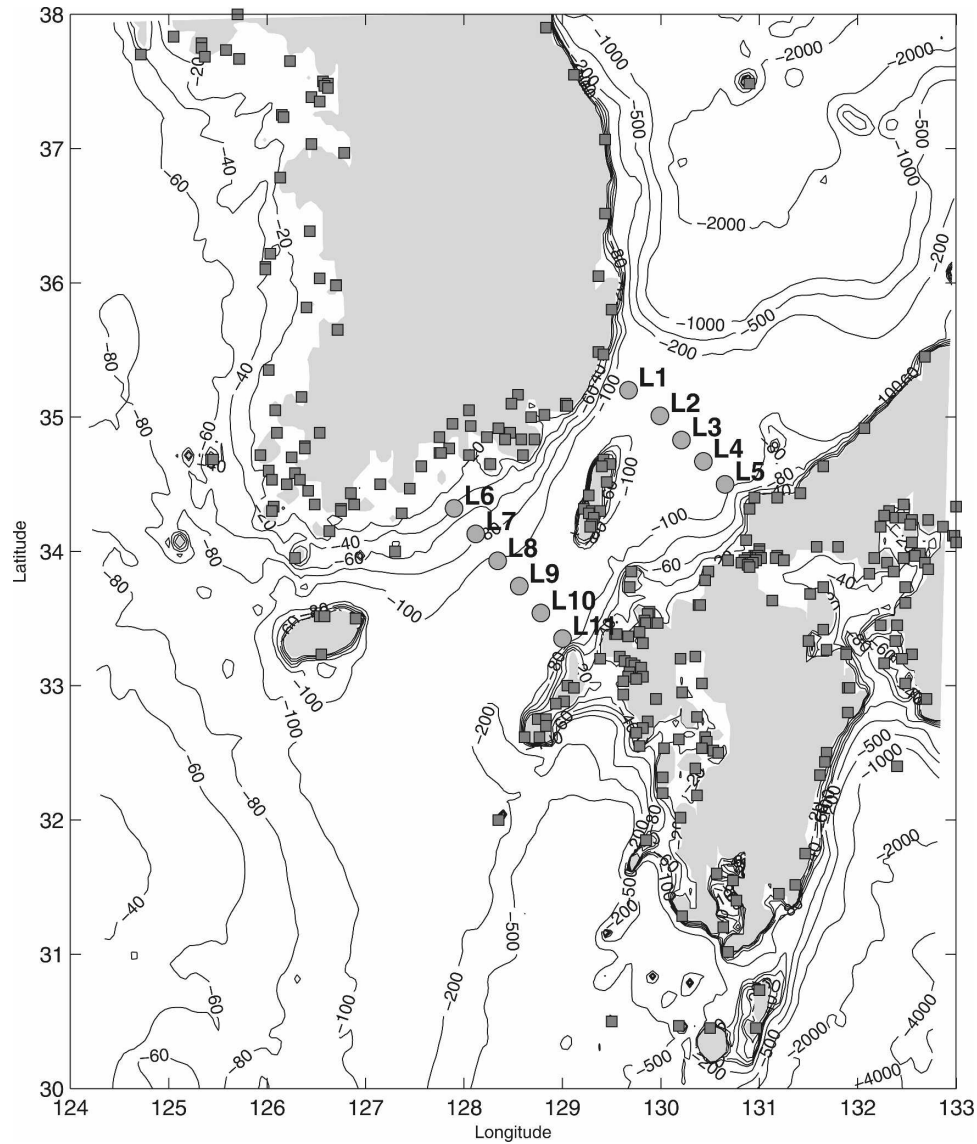


FIG. 5. Bathymetry (m) of the Korean Strait. Squares indicate the IHO stations and circles indicate the location of bottom-mounted ADCPs.

data and the other did not. The resolution of the PCTides grid was 10 km.

Figure 3 shows a comparison of water-level elevation for the data assimilative case versus the observations. Stations 1–3 show tidal ranges of  $\sim 2$  m, while station 4 (the shallowest location and closest to the shore) depicts a range of almost 4 m. Table 1a presents the water-level elevation statistics calculated using the model forecasts with and without data assimilation versus the observations. In general, the statistics for the water-level elevation using data assimilation showed a slight improvement ranging from 2% to 13% over the results without data assimilation. On average, the RMSE is

lower, while the  $R$  and  $SS$  are slightly higher in the data assimilation case. In addition, the average phase lag, calculated as the average of absolute values, is 9 min less in the data assimilation case.

The depth-averaged tidal currents from the PCTides forecasts were compared against the depth-averaged ADCP observations. Figures 4a,b show comparisons of the depth-averaged  $u$ - and  $v$ -velocity components of the ADCPs versus PCTides with data assimilation for the full 30-day period. The phases compare well quantitatively at all four stations. Stations 1 and 2 show periods of small over- or underprediction for the  $u$  and  $v$  components while stations 3 and 4 show overprediction of

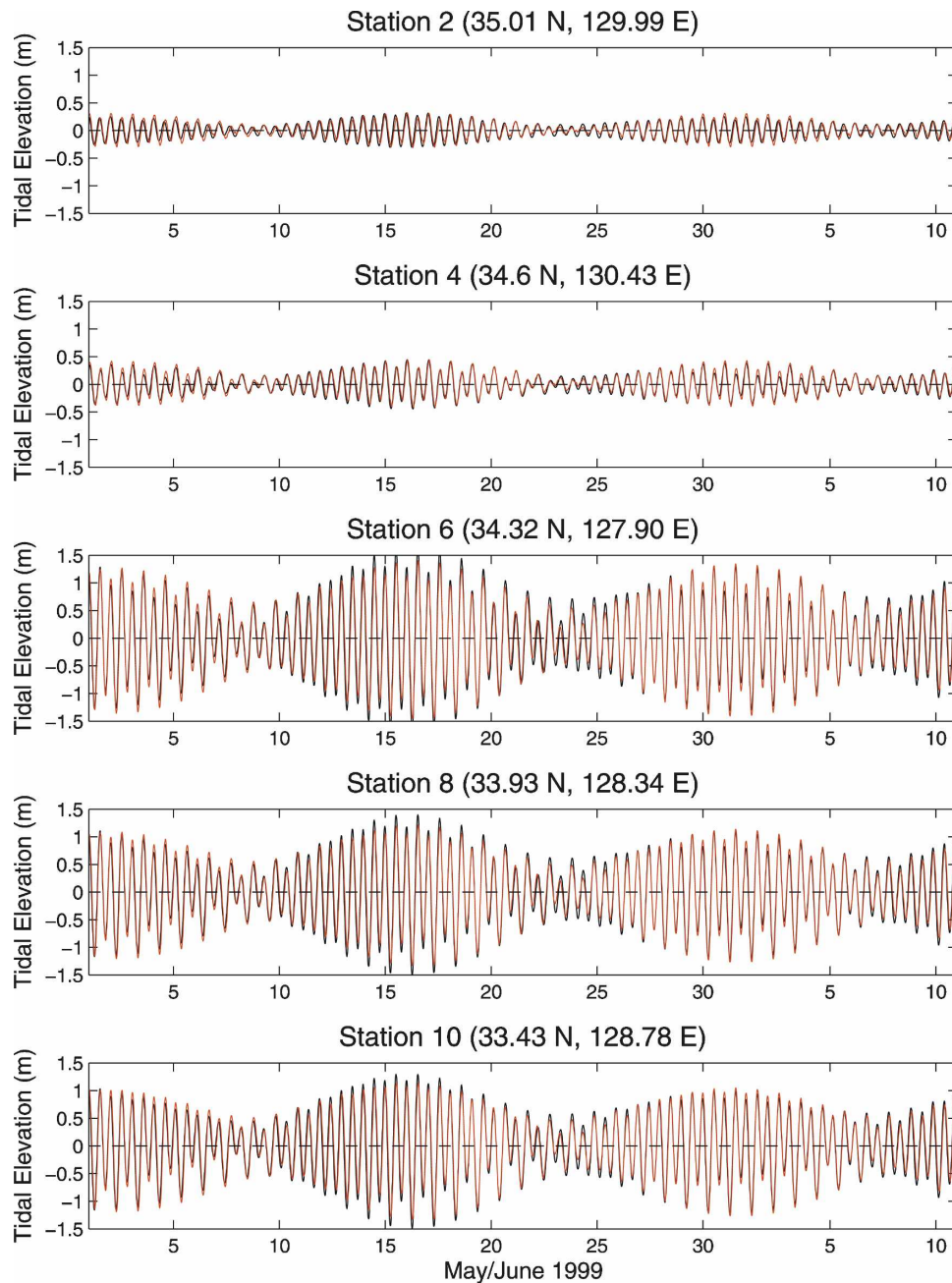


FIG. 6. Korean Straits PCTides water-level elevation forecast (red; m) with data assimilation vs the ADCP (black) at stations L2, L4, L6, L8, and L10 for the period 1–11 Jun 1999.

the  $u$  component and underprediction of the  $v$  component.

Overall, the data assimilative case showed a noticeable improvement in  $R$ ,  $SS$ , and lag (see Table 1b). An examination of the average RMSE of the individual  $u$  and  $v$  components showed a decrease of 40% and 24%, respectively, with the inclusion of data. The effect of data assimilation was most pronounced for the average

phase lag of the  $u$  component, with a reduction of 1 h. The  $v$  component showed a lag time reduced from 63 to 45 min. Similar to the water-level elevations, the PCTides tidal current forecasts demonstrated major improvements when data assimilation was applied to the model. Overall, the velocity errors and phase lags are lower, while the  $R$  and  $SS$  are higher at ADCP locations 3 and 4. Water-level elevation statistics for the model

show the same trend at stations 3 and 4. This is most likely due to the complex bathymetry data near the location of ADCPs 1 and 2, which is not resolved by DBDB2 or the 10-km grid.

In general, it is difficult to predict tidal conditions in the Yellow Sea because of its complex bathymetry, semienclosed geometry, and large tidal signals. Taking all of these into consideration, the globally relocatable PCTides model showed remarkable skill for this 30-day period.

#### b. Korea/Tsushima Strait region

The Korea/Tsushima Strait lies between the Republic of Korea and Kyushu, Japan, and is a shallow area with depths of  $\sim 100$  m. Another set of measurements used in the evaluation of the PCTides forecasts was located in this region. Figure 5 shows the positions of 11 bottom-mounted ADCPs deployed for 11 months during 1999–2000 as part of NRL’s Dynamical Linkage of Asian Marginal Seas (LINKS) program (Teague et al. 2000). The moorings were divided into two lines, one on the Japan Sea side of the strait (L1–L5) referred to as the “northeast” line and one on the East China Sea/Yellow Sea side of the strait (L6–L11) referred to as the “southwest” line. A PCTides domain was set up for this region with 4.7-km resolution and run for the period 1 May–11 June 1999. Two test cases of PCTides forecasts were run: with and without data assimilation. No atmospheric forcing was used in either test case.

PCTides forecast water-level elevations and currents were compared to measurements from the ADCPs. Teague et al. (2006) reported larger tidal ranges along the southwest line, with a maximum range of 3.0 versus 0.7 m along the northeast line. Figure 6 shows a 10-day comparison of observations versus PCTides-predicted water-level elevations with data assimilation from a sampling of the moorings (L2, L4, L6, L8, and L10) for the period 1–10 June 1999. Smaller water-level elevations are predicted by PCTides at L2 and L4 (northeast) and larger elevations are seen at L6, L8, and L10 (southwest) in agreement with the observations. The statistics of the water-level elevations for both cases (with and without data assimilation) are shown in Table 2a. The differences between the two regions where the ADCPs were deployed are evidenced by the  $\sigma$  of the data, which ranges from 0.16 m along L1–L5 to 0.61 m along L6–L11. The  $\sigma$  of the model results reproduces this difference. On average, the tidal phase predictions with data assimilation lagged behind the observations by 22 min along the northeast line and by 18 min along the southwest line, compared to 36 min for all stations without data assimilation. For the northeast set of moorings (L1–L5) the data assimilative case showed

TABLE 2a. Statistics for water-level elevation (m) and phase (min) for PCTides for Korean Straits predictions compared to observations.

	With data assimilation						
	Water-level elevation					Phase	
	RMSE	$\sigma_{\text{Mod}}$	$\sigma_{\text{Obs}}$	$R$	SS	$R_p$	Lag
Location 1	0.04	0.11	0.13	0.95	0.89	0.96	–12
Location 2	0.05	0.13	0.15	0.95	0.90	0.97	–24
Location 3	0.05	0.16	0.16	0.95	0.91	0.98	–24
Location 4	0.05	0.18	0.18	0.96	0.91	0.98	–24
Location 5	0.07	0.22	0.20	0.96	0.88	0.98	–24
Average	0.05	0.16	0.16	0.95	0.90	0.97	22*
Location 6	0.14	0.65	0.67	0.98	0.96	0.98	–12
Location 7	0.13	0.61	0.63	0.98	0.96	0.98	–12
Location 8	0.13	0.58	0.60	0.98	0.95	0.99	–12
Location 9	0.13	0.56	0.58	0.98	0.95	0.99	–24
Location 10	0.13	0.56	0.58	0.97	0.95	0.99	–24
Location 11	0.14	0.57	0.58	0.97	0.94	0.99	–24
Average	0.13	0.59	0.61	0.98	0.95	0.99	18*
Without data assimilation							
	RMSE	$\sigma_{\text{Mod}}$	$\sigma_{\text{Obs}}$	$R$	SS	$R_p$	Lag
Location 1	0.07	0.17	0.13	0.93	0.74	0.98	–36
Location 2	0.07	0.18	0.15	0.93	0.76	0.98	–36
Location 3	0.07	0.20	0.16	0.94	0.79	0.98	–36
Location 4	0.07	0.21	0.18	0.95	0.84	0.98	–36
Location 5	0.08	0.23	0.20	0.95	0.85	0.98	–36
Average	0.07	0.20	0.16	0.94	0.80	0.98	36*
Location 6	0.33	0.86	0.67	0.94	0.75	0.99	–36
Location 7	0.30	0.80	0.63	0.94	0.77	0.99	–36
Location 8	0.27	0.75	0.60	0.95	0.80	0.99	–36
Location 9	0.25	0.72	0.58	0.95	0.81	0.99	–36
Location 10	0.25	0.71	0.58	0.95	0.82	0.99	–36
Location 11	0.25	0.72	0.58	0.95	0.81	0.99	–36
Average	0.24	0.76	0.61	0.95	0.79	0.99	36*

The asterisk (\*) denotes absolute mean.

some improvement in RMSE,  $\sigma$ ,  $R$ , SS, and phase lag. However, the southwest set of measurements (L6–L11) showed a much more pronounced improvement with data assimilation indicated by a 46% reduction in RMSE, 22% reduction in  $\sigma$ , 20% improvement in SS, and 50% reduction in phase lag. This improvement can be attributed in part to the larger number of IHO stations located near the southwest line versus the northeast line, resulting in overall better agreement with the depth-averaged ADCPs.

Figures 7a,b depict comparisons of depth-averaged ADCP currents (both  $u$  and  $v$  components) at stations L3 and L8 for cases with and without data assimilation. At L3, when data assimilation is included, the  $u$  component of velocity is underpredicted in the westward flow, while at L8 the data assimilation shows an overall better comparison with data. Table 2b shows the statistical comparison of the observed versus the predicted

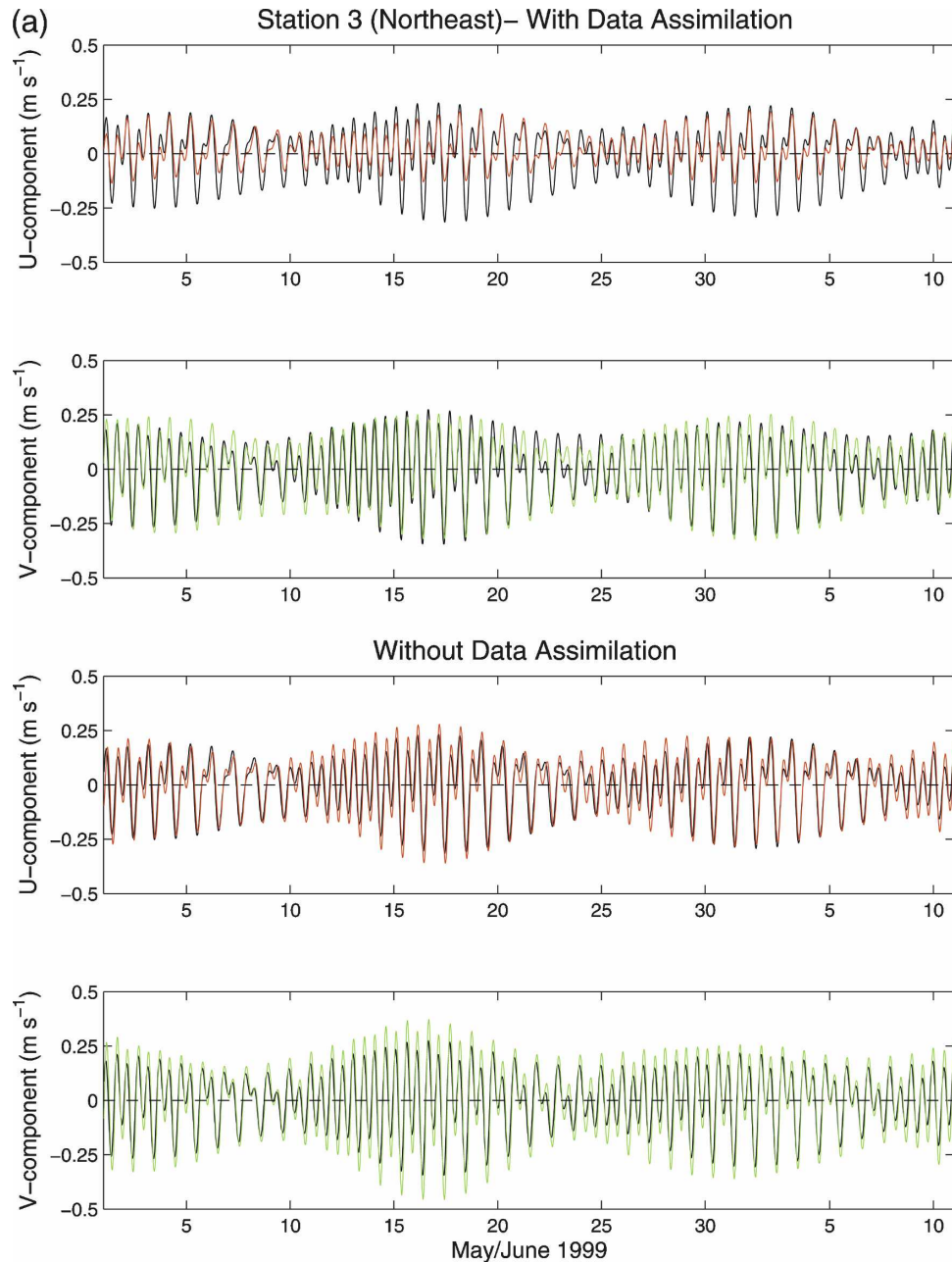


FIG. 7. (a) Korean Straits PCTides depth-averaged tidal current forecasts ( $u$  and  $v$  components;  $\text{m s}^{-1}$ ) with and without data assimilation vs the depth-averaged ADCP observations (black) at station 3 for the period 1 May–11 Jun 1999. (b) Korean Straits PCTides depth-averaged tidal current forecasts ( $u$  and  $v$  component;  $\text{m s}^{-1}$ ) with and without data assimilation vs the depth-averaged ADCP observations (black) at station 8 for the period 1 May–11 Jun 1999.

tidal currents generated with and without data assimilation. Book et al. (2004) found inaccurate bottom-depth values near the L6 mooring when using the Sung Kyun Kwan University (Choi 1999) dataset, which is included in the PCTides bathymetry. As a result, the L6 values are shown but not used in the averaged statistics. The average statistics for the  $u$  and  $v$  components show

a lower RMSE along the southwest line than along the northeast line. In addition, except for the  $v$  component in the data assimilative case, the phase lag is smaller along the southwest line. Statistics for the southwest line are, on average, improved in the data assimilation case. Statistics along the northeast line are slightly degraded in the data assimilative case.

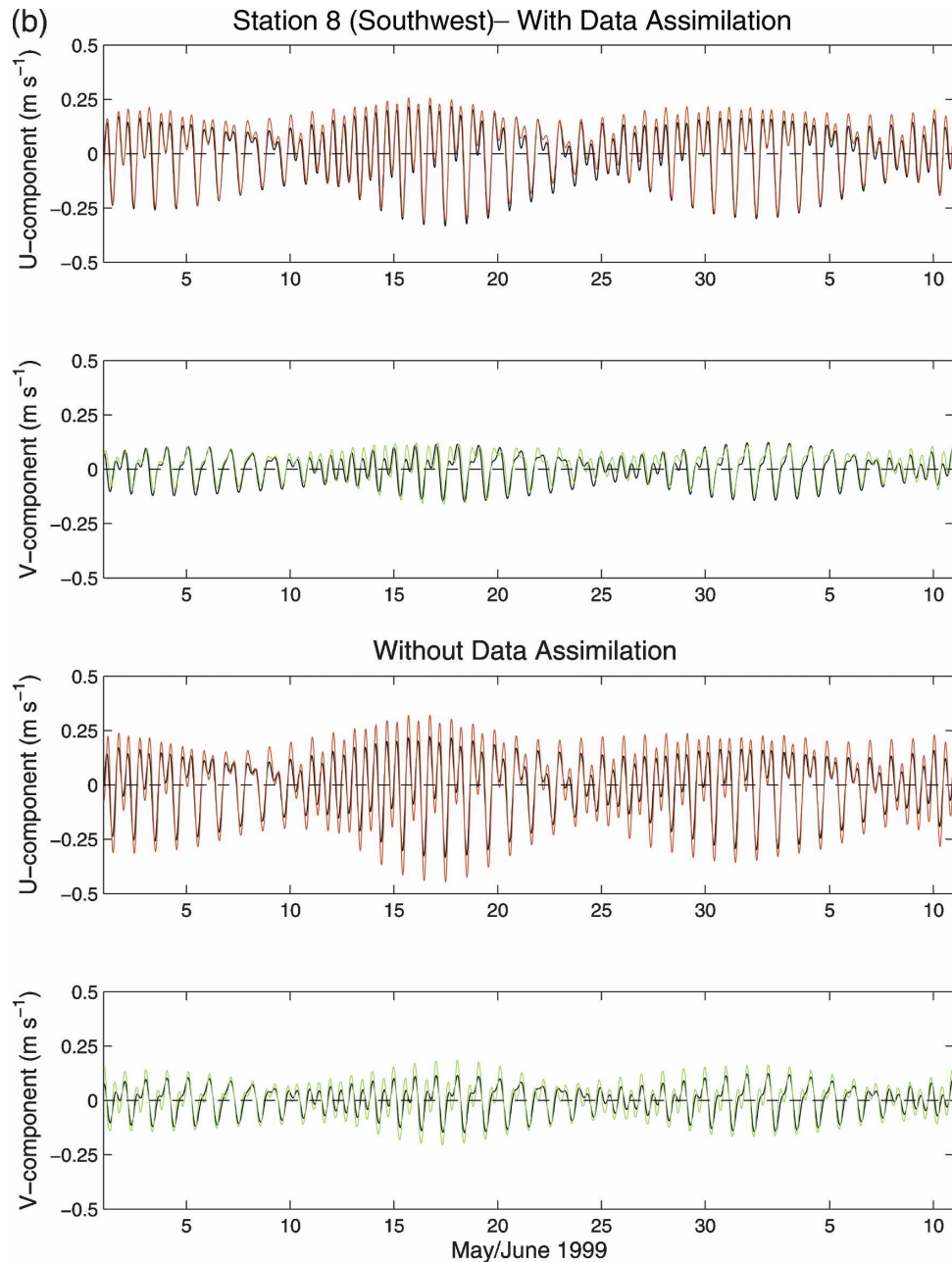


FIG. 7. (Continued)

As an oceanographic constriction or chokepoint between two seas, the Korea Strait is a challenging location for the prediction of tides. The region, one of complex bathymetry and geometry, has been observed to have two distinct tidal conditions: strong tides on the East China Sea/Yellow Sea side and weak tides on the Japan Sea side. During this 42-day period, the PCTides forecast water-level elevation was able to duplicate these conditions. In addition, the PCTides currents, with average RMSE ranging from 0.03 to 0.07  $\text{m s}^{-1}$

and average phase lags ranging from 10 to 67 min, captured key features of the observed currents when compared to the two lines of ADCP observations.

### c. Washington State region

During June 2005, the U.S. Navy conducted an Autonomous Undersea Vehicle Demonstration (AUVFest 2005), held at the U.S. Navy Undersea Warfare Center in Keyport, Washington. During this real-time demonstration, NAVOCEANO performed the of-

TABLE 2b. Statistics of tidal  $u$  and  $v$  components ( $\text{m s}^{-1}$ ) and phase (min) for PCTides Korean Straits predictions compared to observations.

With data assimilation														
	$U$ ( $\text{m s}^{-1}$ )					$U$ phase		$V$ ( $\text{m s}^{-1}$ )					$V$ phase	
	RMSE	$\sigma_{\text{Mod}}$	$\sigma_{\text{Obs}}$	$R$	SS	$R_p$	Lag (min)	RMSE	$\sigma_{\text{Mod}}$	$\sigma_{\text{Obs}}$	$R$	SS	$R_p$	Lag (min)
Location 1	0.05	0.11	0.12	0.94	0.86	0.96	-24	0.07	0.21	0.16	0.96	0.78	0.97	-24
Location 2	0.06	0.09	0.12	0.90	0.76	0.93	-36	0.06	0.16	0.15	0.94	0.86	0.96	-24
Location 3	0.06	0.07	0.12	0.90	0.71	0.91	-12	0.06	0.14	0.13	0.89	0.75	0.95	-48
Location 4	0.07	0.06	0.11	0.88	0.64	0.90	36	0.06	0.13	0.12	0.92	0.78	0.97	-48
Location 5	0.10	0.09	0.12	0.69	0.33	0.92	96	0.06	0.12	0.13	0.92	0.78	0.96	-36
Average	0.07	0.08	0.12	0.86	0.66	0.92	41*	0.06	0.15	0.14	0.93	0.79	0.96	36*
Location 6**	0.04	0.18	0.16	0.98	0.93	0.98	0	0.04	0.05	0.05	0.69	0.33	0.80	96
Location 7	0.03	0.14	0.14	0.98	0.94	0.99	-12	0.03	0.04	0.05	0.83	0.65	0.84	-36
Location 8	0.04	0.13	0.12	0.98	0.91	0.99	-12	0.03	0.06	0.06	0.89	0.72	0.95	-60
Location 9	0.02	0.11	0.12	0.98	0.96	0.99	-24	0.04	0.07	0.08	0.86	0.71	0.98	-84
Location 10	0.02	0.10	0.09	0.99	0.94	0.99	-12	0.04	0.08	0.09	0.90	0.81	0.99	-72
Location 11	0.02	0.12	0.11	0.98	0.96	0.98	0	0.06	0.09	0.09	0.83	0.63	0.99	-84
Average	0.03	0.12	0.12	0.98	0.94	0.99	10*	0.04	0.07	0.07	0.86	0.70	0.95	67*
Without data assimilation														
	$U$ ( $\text{m s}^{-1}$ )					$U$ phase		$V$ ( $\text{m s}^{-1}$ )					$V$ phase	
	RMSE	$\sigma_{\text{Mod}}$	$\sigma_{\text{Obs}}$	$R$	SS	$R_p$	Lag (min)	RMSE	$\sigma_{\text{Mod}}$	$\sigma_{\text{Obs}}$	$R$	SS	$R_p$	Lag (min)
Location 1	0.06	0.15	0.12	0.92	0.74	0.99	-48	0.10	0.23	0.16	0.94	0.63	0.99	-36
Location 2	0.06	0.14	0.12	0.92	0.75	0.98	-48	0.06	0.19	0.15	0.97	0.86	0.99	-24
Location 3	0.05	0.13	0.12	0.91	0.79	0.97	-48	0.06	0.17	0.13	0.94	0.76	0.99	-36
Location 4	0.05	0.12	0.11	0.92	0.84	0.96	-48	0.05	0.15	0.12	0.95	0.81	0.99	-36
Location 5	0.06	0.14	0.12	0.92	0.75	0.97	-48	0.05	0.15	0.13	0.94	0.84	0.98	-36
Average	0.06	0.14	0.12	0.92	0.77	0.97	48*	0.06	0.18	0.14	0.95	0.78	0.99	34*
Location 6**	0.10	0.24	0.16	0.96	0.62	0.97	-12	0.11	0.10	0.05	-0.04	-4.13	0.40	-192
Location 7	0.06	0.19	0.14	0.97	0.79	0.98	-24	0.07	0.08	0.05	0.53	-0.96	0.58	72
Location 8	0.05	0.16	0.12	0.97	0.80	0.98	-24	0.03	0.08	0.06	0.92	0.70	0.93	24
Location 9	0.03	0.13	0.12	0.97	0.93	0.99	-24	0.02	0.09	0.08	0.98	0.92	0.98	-12
Location 10	0.02	0.11	0.09	0.99	0.94	0.99	-12	0.02	0.10	0.09	0.97	0.93	0.97	0
Location 11	0.04	0.12	0.11	0.95	0.89	0.99	48	0.03	0.11	0.09	0.98	0.91	0.98	-24
Average	0.04	0.14	0.12	0.97	0.87	0.98	24*	0.03	0.09	0.07	0.88	0.50	0.89	26*

The asterisk (\*) denotes absolute mean. The double asterisk (\*\*) denotes that the station is not used in average.

ficial operational testing (OPTTEST) of the PCTides system. At the end of the evaluation period, the model output was quantitatively compared to the ADCP observations collected during the exercise. Prior to the OPTTEST, evaluation criteria defining acceptable forecast errors were established for PCTides to meet in order to be declared successful. These criteria included 1) the RMSE of PCTides-predicted water-level elevation versus IHO or the ADCP amplitudes relative to mean sea level must be less than 0.30 m, 2) the RMSE of PCTides-predicted phase versus IHO or the ADCP phase must be less than 30 min (use peak amplitude times only), and 3) the RMSE of current magnitude must be equal to or less than  $0.5 \text{ m s}^{-1}$ .

From 6 to 16 June 2005, the PCTides system forecasted water-level elevations and depth-averaged currents in the Washington State area. The first grid covered all of Puget Sound with a resolution of 12 km (Fig.

8a). A higher-resolution nested grid was run daily with a resolution of 1.5 km (Fig. 8b). Three test cases were run: 1) with data assimilation, 2) without data assimilation, and 3) with assimilation and atmospheric wind/pressure. FES99 tidal constituents were applied as lateral boundary conditions to the PCTides large outer grid (Fig. 8a) while the nest received boundary conditions from the outer grid (12 km). The bathymetry utilized for AUVFest 2005 included NRL's DBDB2 and a high-resolution 3-s bathymetry provided by NAVOCEANO. PCTides software was used to blend these datasets to produce an improved bathymetry and provide more accurate model forecasts.

Similar to the Yellow Sea and Korea Straits test cases, PCTides simulations were performed with and without data assimilation. Additional tests were run to investigate the effect of wind forcing with differing spatial resolution. Winds used during these tests were

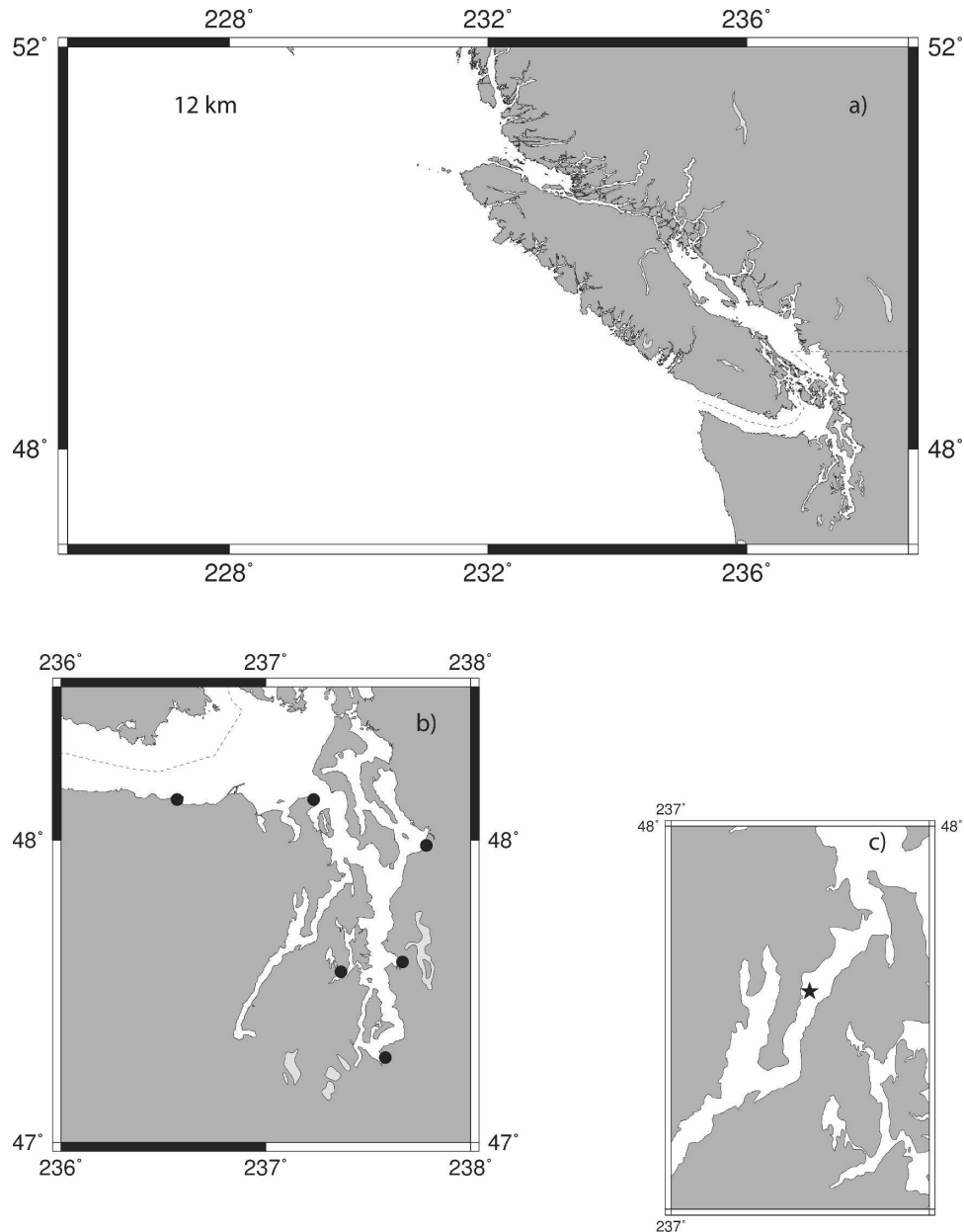


FIG. 8. (a) Host grid resolution of 12 km. (b) Nest1 grid resolution of 1.5 km with IHO stations shown and (c) zoomed area of the Hood Canal with ADCP shown.

from the COAMPS model available at resolutions of 27 km (a standard operational resolution) and a higher resolution of 5 km (typically available only by special request). Our testing showed that the most accurate forecasts were made utilizing winds from the higher-resolution (5 km) test case. Subsequently, only the higher-resolution wind case results will be shown.

The validation data used in this study are from an ADCP deployed in the Hood Canal by NAVOCEANO during the period 7–18 June 2005. The ADCP data in-

dicated that the tidal range in this region was greater than 4 m. Figure 9 depicts a water-level comparison of observations versus the model forecasts for three test cases: 1) without data assimilation or wind, 2) with data assimilation and no wind, and 3) with data assimilation and wind. Table 3a presents water-level elevation statistics for these three test cases. The wind test case showed the best overall skill with an RMSE of 0.16 m, which is impressive considering the tidal range in this region was greater than 4 m. The  $R_p$  for the winds case was 0.99 with a lag of 20 min. While the data assimila-

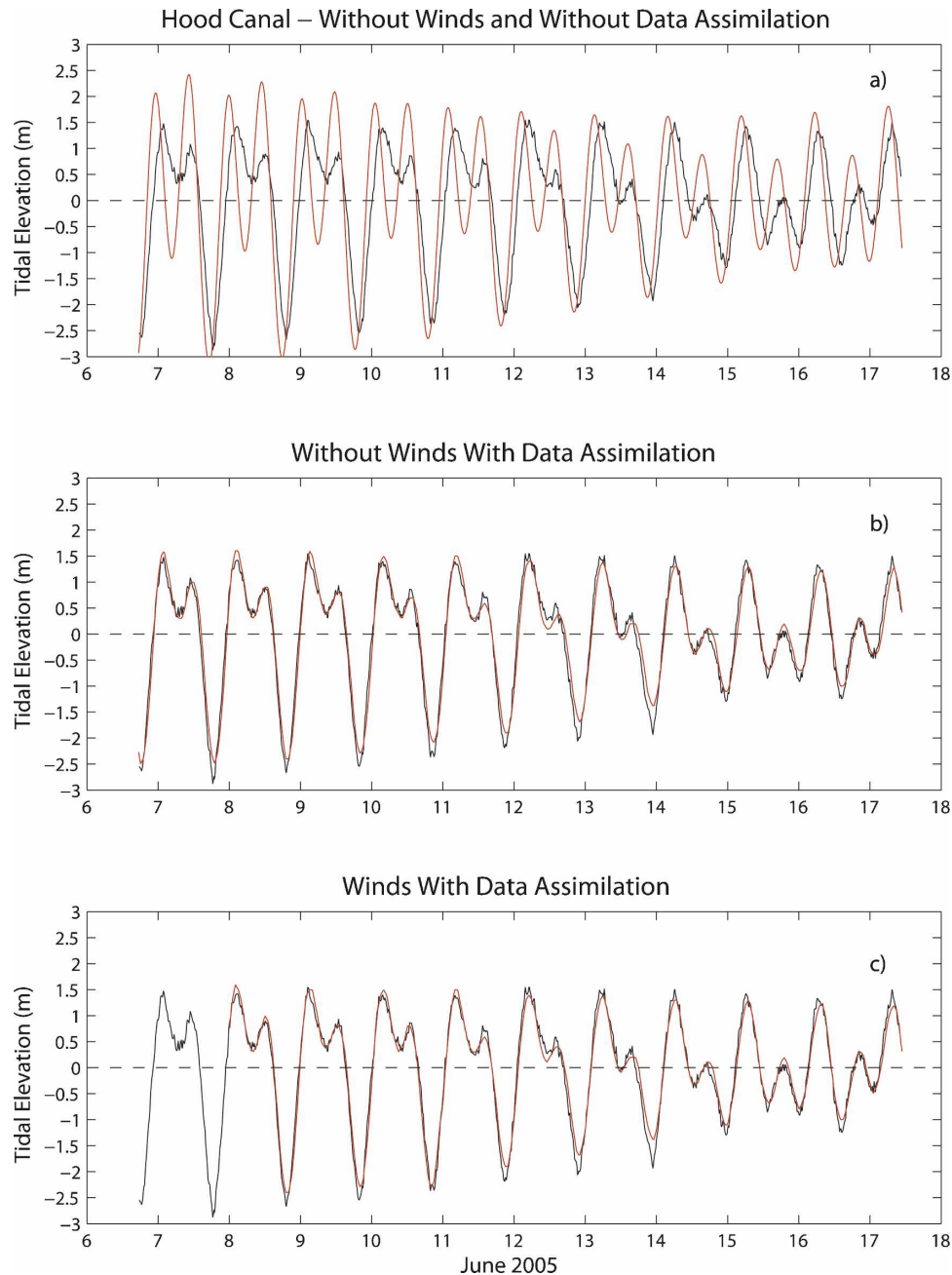


FIG. 9. Water-level elevation (m) comparisons of Hood Canal ADCP (black) vs PCTides forecasts (red) using (a) no wind and no data assimilation, (b) no wind and data assimilation, and (c) wind and data assimilation. The plot is valid 6–17 Jun 2005. PCTides grid resolution is 1.5 km. The wind and data assimilation case started 1 day later than the other two cases.

tion cases compared well against the observations, the study without data assimilation did poorly. The RMSE was  $\sim 1$  m while the  $R$  and  $SS$  were low. In these test cases, the PCTides output frequency was chosen to be 20 min; as a result, a smaller phase lag could not be resolved.

PCTides also forecast tidal current magnitudes dur-

ing AUVFest 2005 as part of the operational evaluation criteria discussed previously. The tidal current magnitude comparison between the ADCP and the PCTides forecast from the 1.5-km grid using 1) no wind and data assimilation and 2) COAMPS wind with data assimilation is shown in Fig. 10. The statistics for both cases are very similar. The RMSE with the inclusion of wind was

TABLE 3a. Statistics of water-level elevation (m) and phase (min) for PCTides Hood Canal predictions compared to observations.

With data assimilation						
Water-level elevation					Phase	
RMSE	$\sigma_{\text{Mod}}$	$\sigma_{\text{Obs}}$	$R$	SS	$R_p$	Lag
Hood Canal with wind						
0.16	0.95	1.05	0.99	0.97	0.99	20
Hood Canal without wind						
0.20	1.00	1.05	0.98	0.96	0.99	20
Without data assimilation						
RMSE	$\sigma_{\text{Mod}}$	$\sigma_{\text{Obs}}$	$R$	SS	$R_p$	Lag
Hood Canal without wind						
0.95	1.28	1.05	0.69	0.20	0.87	96

0.05 m s<sup>-1</sup> and without was 0.06 m s<sup>-1</sup>. The  $R$  for both cases was 0.84.

During AUVFest 2005, PCTides forecasts were used to provide an optimum dive window in two recovery missions (a buoy and a bottom crawler). Unfortunately, because of poor visibility, the buoy was not rescued. A bottom crawler, which had become stuck in the mud, was successfully recovered. Afterward, the feedback from the divers was that the PCTides model forecasts were “dead on.” In addition to this feedback, the statistical comparison calculated from the PCTides forecasts versus the observations was used to determine that PCTides met all the OPTTEST criteria and was declared operational by NAVOCEANO.

Although not part of the PCTides AUVFest evaluation criteria, we examined the  $u$  and  $v$  components of the depth-averaged current from the model versus the depth-averaged ADCP currents (similar to the comparisons discussed earlier for the Yellow Sea and Korean straits). The Hood Canal presents a challenging environment for tidal prediction with a narrow channel and limited IHO stations for data assimilation (see Fig. 8b). Figure 11 depicts comparisons of the depth-averaged ADCP currents (both  $u$  and  $v$  components) at the Hood Canal location for all three PCTides cases. Table 3b shows the statistical comparison of the  $u$  and  $v$  components of the PCTides depth-averaged current versus the observation of the Hood Canal ADCP. Both the  $u$  and  $v$  components from the data assimilation and wind case had high  $R$  and SS values with a phase lag of 0 min. The case with data assimilation but without wind had higher RSME and lower SS than the previous case. Similar to the statistics for the water-level elevation, the velocity statistics for the case without data assimilation or wind showed the poorest results. These results show the importance of data assimilation in constricted areas as well as wind forcing.

#### d. Other exercises (ASIAEX and MREA04)

During the spring of 2001, the Asian Seas International Acoustics Experiment (ASIAEX) took place in the South and East China Seas. To study soliton generation near the Luzon Strait, Ramp et al. (2004) ran PCTides and compared water-level elevations to observations at two locations. The model was run for an area from 15°–26°N, 115°–125°E and assimilated data from 54 IHO stations. In this earlier version of the model, FES95.1/2.1 (Shum et al. 1997) was used to provide lateral boundary conditions. The authors found excellent agreement in water-level elevations during the period 22 April–19 May 2001 with an RMSE of 0.15 m. The authors also compared the PCTides results against the Oregon State University TOPEX/Poseidon global inverse solution (Egbert et al. 1994) and found that PCTides produced “virtually identical results” in the examination of water-level elevations for the area of interest.

PCTides was the tidal prediction component of NRL’s wave, tide, and current prediction system used during the NATO Maritime Rapid Environmental Assessment (MREA04) trial held in Portuguese coastal waters near Pinheiro da Cruz during April 2004 (Fig. 12). The PCTides grid was set up in this area with a resolution of 0.05° and provided daily 48-h forecasts of water-level elevations. Wind and sea level pressure from COAMPS (27 km) were used as atmospheric forcing for the daily forecasts. A total of 28 IHO stations were assimilated into the model solutions.

Waves and nearshore currents were measured during MREA04 by deploying a Nortek Vector acoustic velocimeter (N6) in the surf zone. The sensor package included a pressure gauge placed at low tide in 1.5 m of water. Figure 13 shows a scatterplot of water-level elevations from PCTides versus water observations at Pinheiro da Cruz, an area where surf predictions for amphibious landings were being generated during MREA04. The mean water depth from the N6 data was subtracted from the measured water depth to determine the water-level elevation. Since the N6 data were recorded at irregular intervals (60 or 120 min), the PCTides water-level elevations were temporally interpolated to match the N6 observation times. The statistics showed excellent agreement with an RMSE in amplitude of 0.07 m, phase errors less than 15 min, and an  $R$  of approximately 1.0.

## 4. Summary and conclusions

A global tide/surge forecast system, PCTides, has been developed by NRL for the U.S. Navy to predict

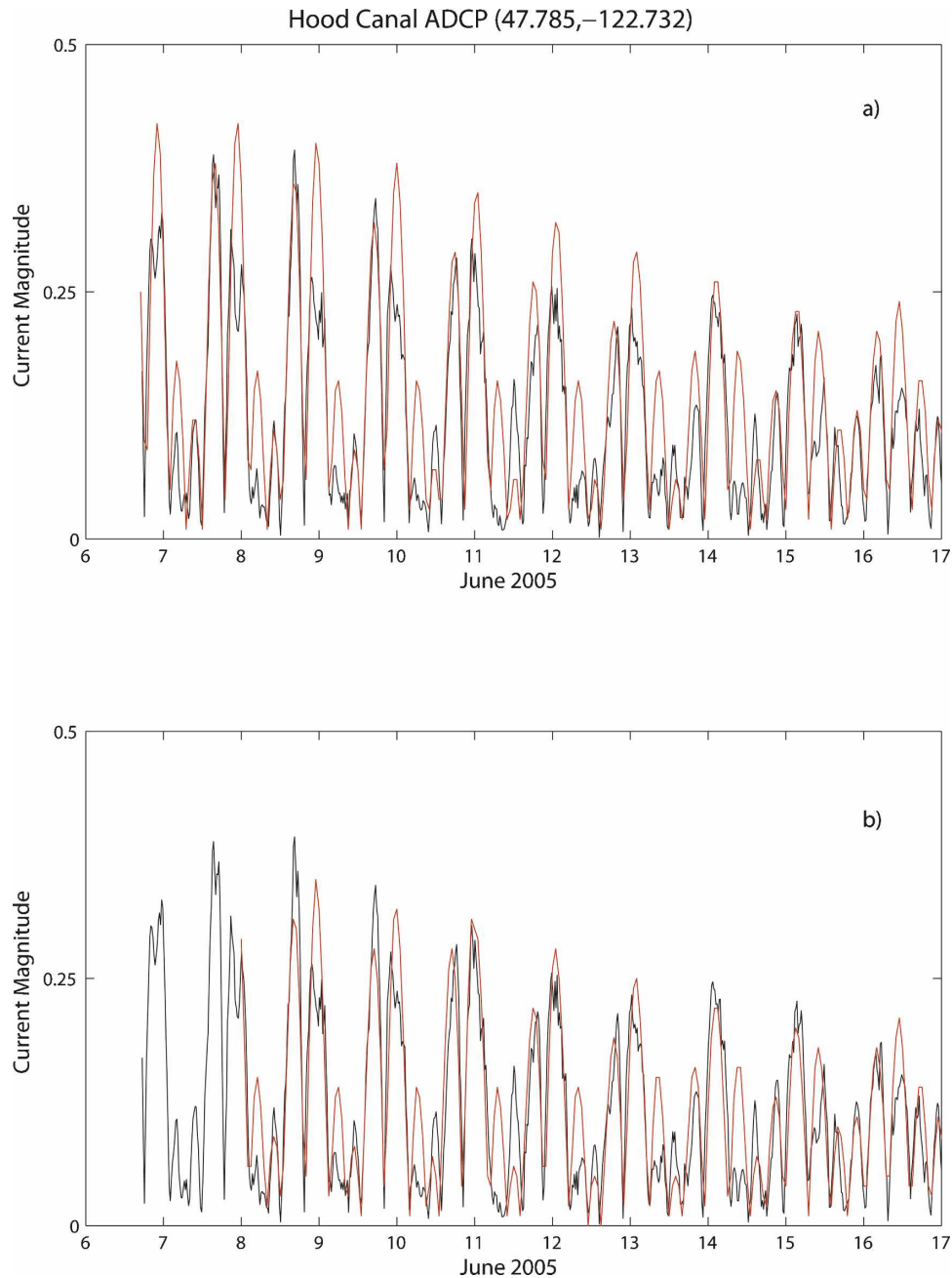


FIG. 10. Tidal current magnitude (m) comparisons of Hood Canal ADCP (black) vs PCTides forecasts (red) using (a) no wind and data assimilation and (b) COAMPS wind and data assimilation. The plot is valid 6–17 Jun 2005. PCTides grid resolution is 1.5 km. The wind and data assimilation case started 1 day later than the other case.

water-level elevation and depth-averaged ocean currents. One of the challenges for the navy is to have the ability to predict water-level elevation and currents for essentially any region worldwide. Tidal prediction in shallow, semienclosed seas and constricted regions such as straits and channels is often more difficult than prediction in open coastal regions. To prove

the global robustness of the PCTides system, it has been evaluated in many different locations by a number of users. This study has focused on three of the more challenging locations for tidal prediction: the shallow, semienclosed Yellow Sea, the Korea Strait, and the Hood Canal. PCTides exhibited skill in prediction of both water-level elevation and tidal currents at

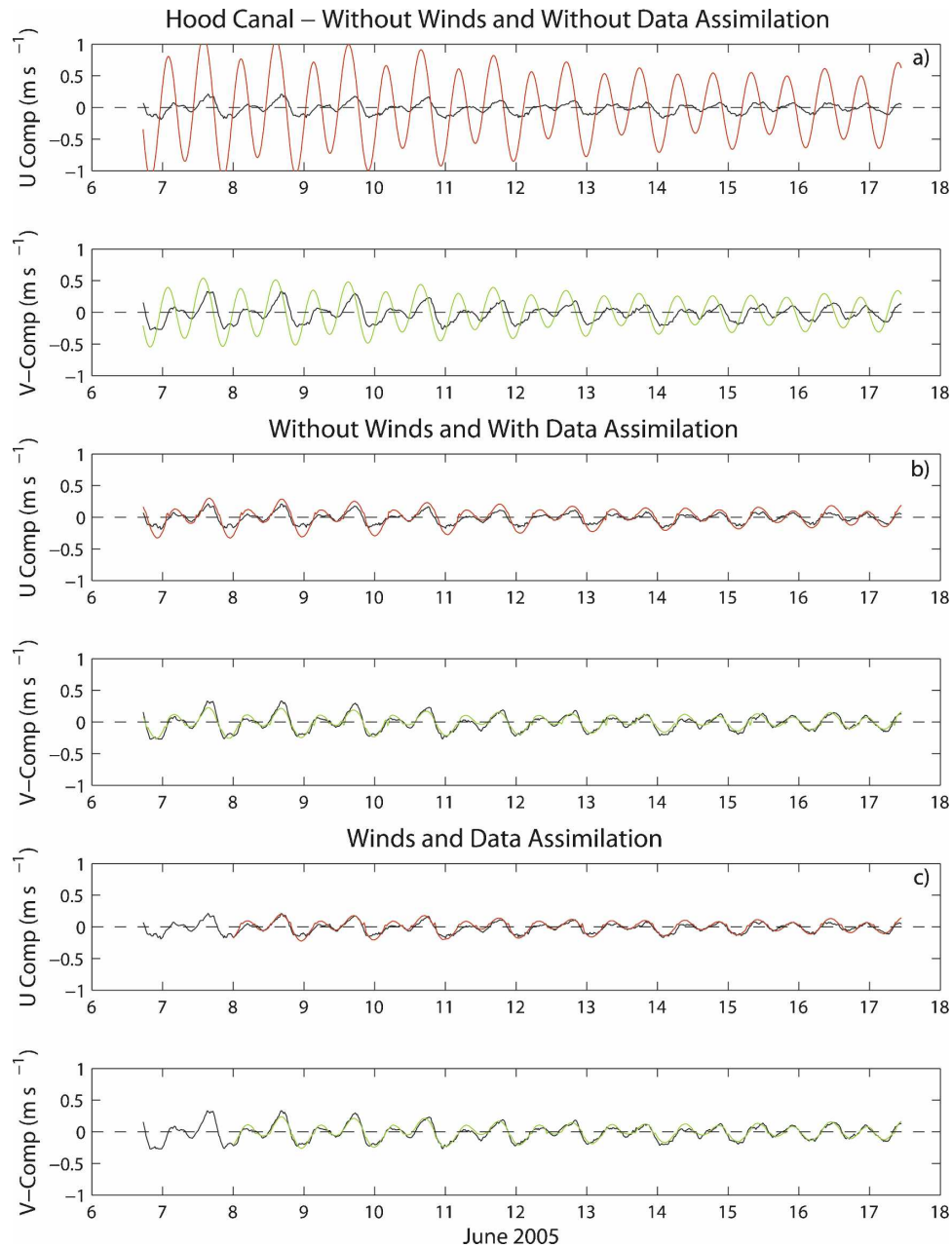


FIG. 11. Hood Canal PCTides depth-averaged tidal current forecasts ( $u$  and  $v$  components;  $\text{m s}^{-1}$ ) with (a) no wind and no data assimilation, (b) no wind and data assimilation, and (c) wind and data assimilation vs the depth-averaged ADCP observation (black) at Hood Canal. The plot is valid 6–17 Jun 2005. PCTides grid resolution is 1.5 km. The wind and data assimilation case started 1 day later than the other two cases.

all three locations. The Hood Canal case was used as the U.S. Navy's operational testing of PCTides. The system easily met the evaluation criteria defined by the U.S. Navy in this location. It was also shown that in these three locations, the PCTides tidal forecasts were improved by assimilating IHO tidal station data. This holds true for most locations in which PCTides has

been tested. This was particularly evidenced in the water-level elevation statistics for the southwest transect in the Korean Straits and Hood Canal where the assimilation of IHO station data showed a marked improvement in model skill. Although this paper focused primarily on the evaluation of PCTides both with and without data assimilation, the Hood Canal test case

TABLE 3b. Statistics of tidal  $u$  and  $v$  components ( $\text{m s}^{-1}$ ) and phase (min) for PCTides Hood Canal predictions compared to observations.

With data assimilation													
$U$ ( $\text{m s}^{-1}$ )					$U$ phase		$V$ ( $\text{m s}^{-1}$ )					$V$ phase	
RMSE	$\sigma_{\text{Mod}}$	$\sigma_{\text{Obs}}$	$R$	SS	$R_p$	Lag (min)	RMSE	$\sigma_{\text{Mod}}$	$\sigma_{\text{Obs}}$	$R$	SS	$R_p$	Lag (min)
Hood Canal with wind													
0.04	0.09	0.07	0.92	0.71	0.93	0	0.04	0.11	0.11	0.94	0.89	0.94	0
Hood Canal without wind													
0.07	0.14	0.12	0.93	0.18	0.93	20	0.05	0.11	0.12	0.93	0.86	0.93	0
Without data assimilation													
$U$ ( $\text{m s}^{-1}$ )					$U$ Phase		$V$ ( $\text{m s}^{-1}$ )					$V$ phase	
RMSE	$\sigma_{\text{Mod}}$	$\sigma_{\text{Obs}}$	$R$	SS	$R_p$	Lag (min)	RMSE	$\sigma_{\text{Mod}}$	$\sigma_{\text{Obs}}$	$R$	SS	$R_p$	Lag (min)
Hood Canal without wind													
0.50	0.53	0.08	0.53	-38.31	0.86	120	0.22	0.26	0.12	0.52	-2.19	0.89	120

showed that the inclusion of wind forcing added to the forecast skill.

This study has illustrated the importance of accurate bathymetry as well as the value of data assimilation in tidal prediction. Although the globally relocatable PC-

Tides system has been proven to be a skillful tool for tidal prediction, continued feedback from users of the system and subsequent model enhancements will further improve the system's accuracy.

*Acknowledgments.* The authors thank Dr. William Teague and Dr. Jeffery Book (NRL) for providing ADCP data for the Yellow Sea and Korea Straits regions. We would also like to thank Dr. Frank Bub, Mr. Bryan Mensi, and Dr. Robert Carter (NAVOCEANO) for providing ADCP data and PCTides operational daily forecasts during AUVFest 2005. Also thanks to Mr. Jim Dykes (NRL) for providing PCTides compari-

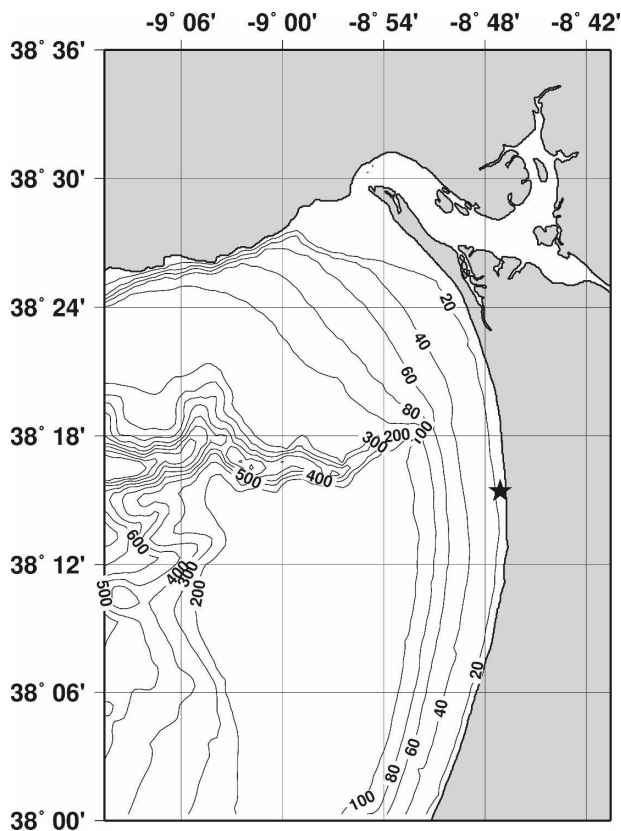


FIG. 12. Bathymetry (m) of MREA04 exercise off the coast of Portugal. The star is the Nortek acoustic velocimeter (N6) near Pinheiro da Cruz.

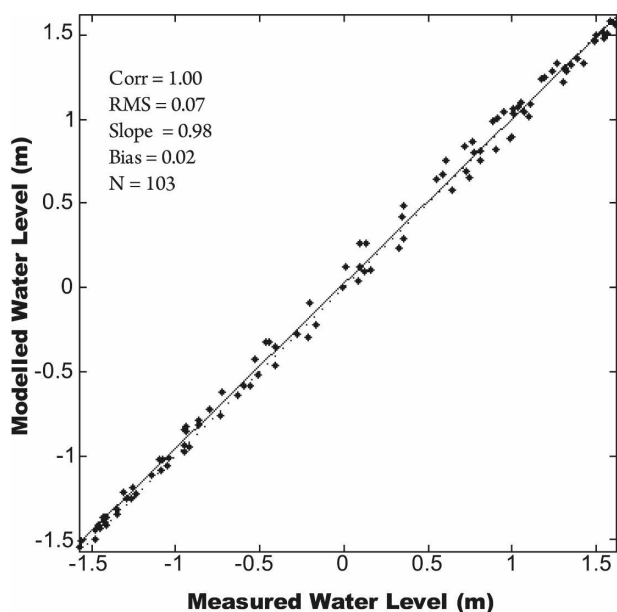


FIG. 13. Portugal area scatterplot of water-level elevation forecasts from PCTides vs observations for April 2004.

son plots from the MREA04 exercise and to the NATO Undersea Research Center (NURC) for providing the near-shore water-level data. Thanks are also extended to Mr. Paul Martin (NRL) and the external reviewers for their helpful suggestions.

## REFERENCES

- Blain, C. A., 1997: Development of a data sampling strategy for semienclosed seas using a shallow-water model. *J. Atmos. Oceanic Technol.*, **14**, 1157–1173.
- , T. C. Massey, J. D. Dykes, and P. G. Posey, 2007: Advanced surge and inundation modeling: A case study from Hurricane Katrina. 2007 Naval Research Laboratory Review, 286 pp.
- Book, J. W., and Coauthors, 2004: Data assimilation modeling of the barotropic tides in the Korea/Tsushima Strait. *J. Oceanogr.*, **60**, 977–993.
- Choi, B. H., 1999: *Digital Atlas for Neighboring Seas of Korean Peninsula*. Laboratory for Coastal and Ocean Dynamics Studies, Sung Kyun Kwan University, CD-ROM.
- Egbert, G. D., A. F. Bennett, and M. G. G. Foreman, 1994: TOPEX/POSEIDON tides estimated using a global inverse model. *J. Geophys. Res.*, **99**, 24 821–24 852.
- Hodur, R. M., 1997: The Naval Research Laboratory's Coupled Ocean/Atmosphere Mesoscale Prediction System (COAMPS). *Mon. Wea. Rev.*, **125**, 1414–1430.
- Hogan, T. F., and T. E. Rosmond, 1991: The description of the Navy Operational Global Atmospheric Prediction System's spectral forecast model. *Mon. Wea. Rev.*, **119**, 1786–1815.
- Holland, G. J., 1980: An analytical model of the wind and pressure profiles in hurricanes. *Mon. Wea. Rev.*, **108**, 1212–1218.
- Hubbert, G. D., L. M. Leslie, and M. J. Manton, 1990: A storm surge model for the Australian region. *Quart. J. Roy. Meteor. Soc.*, **116**, 1005–1020.
- IHO, 1988: Tidal constituent bank station catalogue. Ocean and Aquatic Sciences, Department of Fisheries and Oceans, Ottawa, Canada, Special Publ. 50, 100 pp.
- Jenkins, G. M., and D. G. Watts, 1969: *Spectral Analysis and Its Applications*. Holden-Day, 525 pp.
- Kara, A. B., A. J. Wallcraft, and H. E. Hurlburt, 2003: Climatological SST and MLD predictions from a global layered ocean model with an embedded mixed layer. *J. Atmos. Oceanic Technol.*, **20**, 1616–1632.
- Lefevre, F., F. H. Lyard, and C. Le Provost, 2002: FES99: A global tide finite element solution assimilating tide gauge and altimetric information. *J. Atmos. Oceanic Technol.*, **19**, 1345–1356.
- Messinger, F., and A. Arakawa, 1976: *Numerical Methods Used in Atmospheric Models*. GARP Publication Series 14, WMO/ICSU Joint Organizing Committee, 64 pp.
- Miller, M. J., and R. P. Pearce, 1974: Numerical model of a cumulonimbus. *Quart. J. Roy. Meteor. Soc.*, **100**, 122–154.
- Murphy, A. H., and E. S. Epstein, 1989: Skill scores and correlation coefficients in model verification. *Mon. Wea. Rev.*, **117**, 572–581.
- Posey, P. G., R. H. Preller, and G. M. Dawson, 2006: PCTides validation test report. Naval Research Laboratory Rep. NRL/MR/7320—06-8910, Stennis Space Center, MS, 48 pp.
- Preller, R. H., P. G. Posey, and G. M. Dawson, 2002: The operational evaluation of the Navy's globally relocatable tide model (PCTides). *Mar. Technol. Soc.*, **2**, 847–852.
- , —, and —, 2005: Hurricane Isabel: A numerical study of storm surge along the east coast of the United States. Preprints, *Sixth Conf. on Coastal Atmospheric and Oceanic Prediction and Processes*, San Diego, CA, Amer. Meteor. Soc., P2.9. [Available online at <http://ams.confex.com/ams/pdfpapers/84972.pdf>.]
- Ramp, S., and Coauthors, 2004: Internal solitons in the Northeastern South China Sea Part I: Sources and deep water propagation. *IEEE J. Oceanic Eng.*, **29**, 1157–1181.
- Shum, C. K., and Coauthors, 1997: Accuracy assessment of recent ocean tide models. *J. Geophys. Res.*, **102**, 25 173–25 194.
- Signell, R. P., and B. Butman, 1992: Modeling tidal exchange and dispersion in Boston Harbor. *J. Geophys. Res.*, **97**, 15 591–15 606.
- Smith, S. D., and E. G. Banke, 1975: Variation of the sea surface drag coefficient with wind speed. *Quart. J. Roy. Meteor. Soc.*, **101**, 665–673.
- Teague, W. J., P. Pistek, G. A. Jacobs, and H. T. Perkins, 2000: Evaluation of tides from TOPEX/Poseidon in the Bohai and Yellow Seas. *J. Atmos. Oceanic Technol.*, **17**, 679–687.
- , and Coauthors, 2006: Currents through the Korea/Tsushima Strait: A review of LINKS observations. *Oceanography*, **19** (3), 50–63.